Inorg. Chem. **2009**, *48*, 4108−4117

Stereoselective Formation of Helical Binuclear Metal Complexes: Synthesis, Characterization, and Crystal Structures of Chiral Bis-Rhenium(I) Quaterpyridine Complexes

Ho-Lun Yeung,[†] Wai-Yeung Wong,[‡] Chun-Yuen Wong,[†] and Hoi-Lun Kwong*[,†]

Department of Biology and Chemistry, City University of Hong Kong, Tat Chee Avenue, Kowloon, Hong Kong SAR, China, and Department of Chemistry, Hong Kong Baptist University, Waterloo Road, Hong Kong SAR, China

Received November 22, 2008

A series of single-stranded helical Re(I) complexes, of formula $[Re_2(\mathbf{L})Br_2(CO)_6]$, were prepared by reacting $[Re(CO)_5Br]$ with chiral quaterpyridines **L1**−**4**. By ^1H and ^{13}C NMR analysis, all the crude complexes consisted of a pair of stereoisomers. Sterically more demanding ligand **L4** induced a higher ratio (80:20) than **L1**−**3** (about 56:44). Stereochemically pure complexes could be obtained by recrystallization in CH_2Cl_2. X-ray crystallographic analysis of single crystals from purified complexes showed a single-stranded helical structure with a bridging ligand wrapped around two distorted octahedral rhenium metals, both of which possessed one bromide ligand and three carbonyl ligands in a fac coordination. The helical core is established by extensive noncovalent electrostatic interactions and chiral information is transmitted from the ligand to the helix through these interactions. Solution behavior was studied by CD spectroscopy, and the strong Cotton effect confirms the integrity of the helical structure in solution. The diastereoselectivity of helicates is proposed to be induced by steric interaction between the bromine atom and the substituent of the bridging ligand.

Introduction

The stereoselective formation of chiral supramolecules is of fundamental interest as the interplay between chiral elements of stereogenic carbon and the configuration of metal and secondary/tertiary structures, in higher hierarchical structures, directs the self-assembly process and supramolecular recognition in both chemical and biological systems.[1−4] Supramolecular syntheses, in this aspect, can include components with predetermined stereocenters but can also create new chiral elements at the molecular level.[5]

Helical polynuclear metal complexes,[6,7] one of the paradigmatic branches of supramolecular architecture, consist of chiral components with stereocenters on metals (Δ/λ) and secondary structures (*P*/*M*). The introduction of carbon stereocenters into assembly of helical structures is a common approach to control metal center configuration and ultimately the handedness of the helical configuration.[8,9] The chiral moieties can be introduced into bridging units or extremities of ligands, integrated into ancillary ligands, or introduced into chiral counterions. Most examples have been focused on double- and triple-stranded helicates, and the earliest example is reported by Carrano and Raymond, who used chiral rhodotorulic acid to study the formation of iron triple-stranded helicate.[10] Later Lehn et al. reported stereoselective formation of trinuclear double helicates of Cu(I) and Ag(I) with chiral tris(bipyridines) ligands.[11] Siegel et al. used a chiral dipod as linker to stereoselectively control the helical

* E-mail: bhhoik@cityu.edu.hk.
[†] City University of Hong Kong.
[‡] Hong Kong Baptist University.

(1) Seeber, G.; Tiedemann, B. E. F.; Raymond, K. N. *Top. Curr. Chem.* **2006**, *265*, 147.
(2) Mateos-Timoneda, M.; Crego-Calama, M.; Reinhoudt, D. N. *Chem. Soc. Rev.* **2004**, *33*, 363.
(3) Mamula, O.; von Zelewsky, A. *Coord. Chem. Rev.* **2003**, *242*, 87.
(4) Scarso, A.; Rebek, J., Jr. *Top. Curr. Chem.* **2006**, *265*, 1.
(5) (a) Lehn, J.-M. *Supramolecular Chemistry: Concepts and Perspectives*; VCH: Weinheim, 1995. (b) von Zelewsky, A. *Stereochemistry of Coordination Compounds*; John Wiley & Sons Ltd: Chichester, 1996.
(6) Albrecht, M. *Chem. Rev.* **2001**, *101*, 3457.
(7) Piguet, C.; Bernardinelli, G.; Hopfgartner, G. *Chem. Rev.* **1997**, *97*, 2005.
(8) (a) Von Zelewsky, A. *Coord. Chem. Rev.* **1999**, *190*−*192*, 811. (b) Knof, U.; Von Zelewsky, A. *Angew. Chem.* **1999**, *111*, 312. (c) Knof, U.; Von Zelewsky, A. *Angew. Chem. Int. Ed.* **1999**, *38*, 302.
(9) He, C.; Zhao, Y.; Guo, D.; Lin, Z.; Duan, C. *Eur. J. Inorg. Chem.* **2007**, 3451.
(10) Carrano, C. J.; Raymond, K. N. *J. Am. Chem. Soc.* **1978**, *100*, 5371.
(11) Zarges, W.; Hall, J.; Lehn, J.-M. *Helv. Chim. Acta* **1991**, *74*, 1843.

10.1021/ic802249f CCC: $40.75
Published on Web 04/07/2009

chirality of helicates.[12] Gelalcha[13] and Constable[14,15] reported chiral pybox, terpyridines, and quaterpyridines respectively for diastereoselective formation of a dinuclear double helix. Von Zelewsky developed a family of CHIRAGEN ligands which form chiral double, triple, and circular helicates.[16] Albrecht and co-workers also studied different chiral ligands in the selective formation of triple-stranded helicates.[17]

Although single-stranded helicates have been reported[18] and proposed as initial intermediates[19] for the binding of second and third strands in formation of double- and triple-stranded helicates, very little attention has been focused on their stereoselective formation and potential applications. Elucidating the mechanism of the self-assembly process of the chiral single-stranded helicate and developing stereoselective synthesis can potentially lead to useful applications. For example, optically pure helicates may serve as chiral templates for chiral recognition. They can act as building blocks in the preparation of stereochemically well-defined helical supramolecular structures, reducing the number of stereoisomers presented in the process. In addition, they are also potential chiral catalysts for asymmetric catalysis.

Recently, we obtained stereoselectively, through the use of chiral quaterpyridines, dinuclear Pd(II) single-stranded helicates, and reported their first attempt in asymmetric allylic alkylation.[20] Continuing our effort in the understanding of polynuclear single-stranded helicates, we herein report the stereoselective formation of rhenium single-stranded helicates with a series of chiral quaterpyridine ligands. Noncovalent interactions, commonly observed in biological systems, were found to be significant in maintaining the stability and integrity of the isolated helix both in solid and solution state.

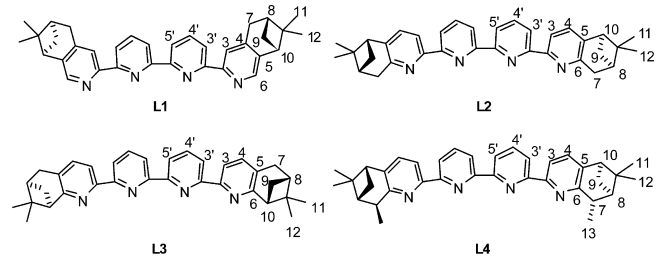

Results

Preparation and Characterization of Chiral Quaterpyridine Ligands. Chiral quaterpyridine ligands **L1**−**4**, which possess a pair of rigid stereogenic cyclic centers bonded to the [4,5] or [5,6] position of terminal pyridine rings, were prepared by a three-step procedure starting from 2-acetyl-6-bromopyridine (Scheme 1).[20] They were readily synthesized by Ni(0)-mediated homocouplings of bipyridines **2a**−**d,** which were obtained in good yield via Kröhnke condensation of pyridinium iodide **1** and different α,β-unsaturated ketones.[21] In both the ^{1}H and ^{13}C NMR spectra, C_2-symmetric pattern are observed for all ligands in solution.

Single crystals suitable for X-ray structure analysis were obtained by evaporation of a concentrated solution of **L4** in CH_2Cl_2. Figure 1a shows the ORTEP diagram of **L4**. The pyridine rings adopt the expected transoid geometry, which is similar to those of 2,2′-bipyridine[22] and 2,2′:6′,2″:6″,2‴-quaterpyridine.[23] The four pyridine rings are approximately trans coplanar to each other. The bond lengths within the molecule closely approximate those observed in achiral quaterpyridine,[23] though the planarity of the ligand is affected by the chiral substituents. With the torsion angles between the pyridyl rings being 3.13°, 16.66°, and 12.27°, in comparison with the linear achiral polypyridine the structure is slightly perturbed by the chiral substituents. The crystal packing of the quaterpyridine molecules in Figure 1b gives a clearer picture of the skewed structure. The interplanar separation of 5.122 Å indicates no significant π−π interaction.

Preparation and Purification of Bis-Rhenium Complexes. The synthesis of rhenium-quaterpyridine complex has been reported previously.[24] As shown in Scheme 2, the single-stranded bis-rhenium(I) complexes [Re_2(**L1**)Br_2(CO)6] (**C1**), [Re_2(**L2**)$Br_2(CO)_6$] (**C2**), [Re_2(**L3**)Br2$(CO)_6$] (**C3**), and [Re_2(**L4**)$Br_2(CO)_6$] (**C4**) were prepared by reacting chiral quaterpyridine ligands with $ReBr(CO)_5$. At refluxing temperature and in a mixture of THF and benzene, ligands **L1**−**4** reacted gradually with rhenium(I) complex to give a good yield of yellow complexes, which were precipitated out of the mixture by adding light petroleum ether. The new

(12) (a) Woods, C. R.; Benaglia, M.; Cozzi, F.; Siegel, J. S. *Angew. Chem.* **1996**, *108*, 1977. (b) Woods, C. R.; Benaglia, M.; Cozzi, F.; Siegel, J. S. *Angew. Chem.* **1996**, *35*, 1830.
(13) Gelalcha, F. G.; Schulz, M.; Kluge, R.; Sieler, J. *J. Chem. Soc., Dalton Trans.* **2002**, 2517.
(14) Constable, E. C.; Kulke, T.; Neuburger, M.; Zehnder, M. *J. Chem. Soc. Chem. Commun.* **1997**, 489.
(15) (a) Baum, G.; Constable, E. C.; Fenske, D.; Kulke, T. *Chem. Commun.* **1997**, 2043. (b) Baum, G.; Constable, E. C.; Fenske, D.; Housecroft, C. E.; Kulke, T. *Chem.—Eur. J.* **1999**, *5*, 1862.
(16) (a) Mamula, O.; von Zelewsky, A.; Bark, T.; Bernardinelli, G. *Angew. Chem.* **1999**, *111*, 3129. Mamula, O.; von Zelewsky, A.; Bark, T.; Bernardinelli, G. *Angew. Chem.* **1999**, *38*, 2945. (b) Mürner, H.; von Zelewsky, A.; Hopfgartner, G. *Inorg. Chim. Acta* **1998**, *271*, 36. (c) Mamula, O.; von Zelewsky, A.; Bernadinely, G. *Angew. Chem.* **1998**, *37*, 289.
(17) Albrecht, M.; Dehn, S.; Raabe, G.; Fröhlich, R. *Chem. Commun.* **2005**, 5690.
(18) (a) Cathey, C. J.; Constable, E. C.; Hannon, M. J.; Tocher, D. A.; Ward, M. D. *J. Chem. Soc. Chem. Commun.* **1990**, 621. (b) Ho, P. K.-K.; Cheung, K.-K.; Peng, S.-M.; Che, C.-M. *J. Chem. Soc., Dalton Trans.* **1996**, 1411. (c) Fu, Y.-J.; Sun, W.-Y.; Dai, W.-N.; Shu, M.-H.; Xue, F.; Wang, D.-F.; Mak, T. C. W.; Tang, W.-X.; Hu, H.-W. *Inorg. Chim. Acta* **1999**, *290*, 127. (d) Ho, P. K.-K.; Peng, S.-M.; Wong, K.-K.; Che, C.-M. *J. Chem. Soc., Dalton Trans.* **1996**, 1829. (e) Chamchoumis, C. M.; Potvin, P. G. *J. Chem. Soc., Dalton Trans.* **1999**, 1373.
(19) (a) Fatin-Rouge, N.; Blanc, S.; Pfeil, A.; Rigault, A.; Albrecht-Gary, A.-M.; Lehn, J.-M. *Helv. Chim. Acta* **2001**, *84*, 1694. (b) Elhabiri, M.; Hamacek, J.; Bünzli, J.-C. G.; Albrecht-Gary, A. M. *Eur. J. Inorg. Chem.* **2004**, 51.
(20) Kwong, H.-L.; Yeung, H.-L.; Lee, W.-S.; Wong, W.-T. *Chem. Commun.* **2006**, 4841.
(21) (a) Kwong, H.-L.; Lee, W.-S. *Tetrahedron: Asymmetry* **2000**, *11*, 2299. (b) Kwong, H.-L.; Wong, W.-L.; Lee, W.-S.; Cheng, L.-S.; Wong, W.-T. *Tetrahedron: Asymmetry* **2001**, *12*, 2683.
(22) Chisholm, M. H.; Huffman, J. C.; Rothwell, I. P.; Bradley, P. G.; Kress, N.; Woodruff, W. H. *J. Am. Chem. Soc.* **1981**, *103*, 3945.
(23) (a) Constable, E. C.; Elder, S. M.; Healy, J.; Tocher, D. A. *J. Chem. Soc., Dalton Trans.* **1990**, 1669. (b) Constable, E. C.; Heirtzler, F.; Neuburger, M.; Zehnder, M. *J. Am. Chem. Soc.* **1997**, *119*, 5606.
(24) Gelling, A.; Orrell, K. G.; Osborne, A. G.; Šik, V. *Polyhedron* **1999**, *18*, 1285.

Scheme 1. Synthesis of Quaterpyridines **L1−4**

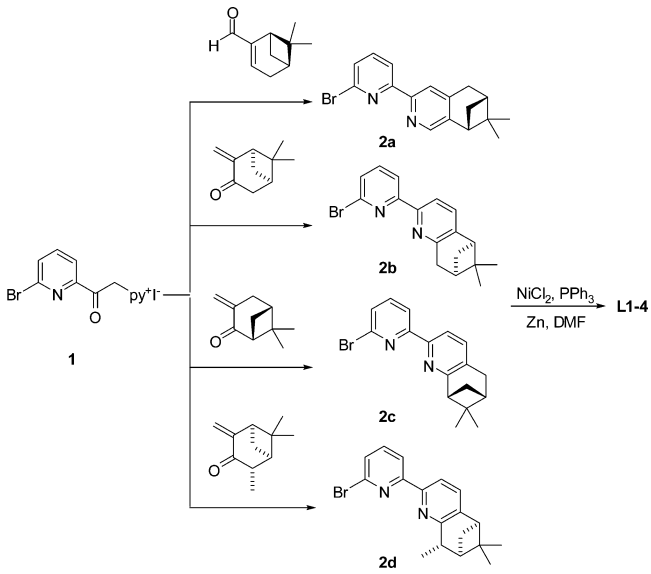

compounds, air-stable in both solid and solution states, while readily soluble in polar solvents, such as CH_2Cl_2, $CHCl_3$, and CH_3OH, are only slightly soluble in diethyl ether and completely insoluble in hexane and light petroleum ether. By elemental analysis, the formula of the crude single-stranded helicates is confirmed to be $[Re_2(\mathbf{L})Br_2(CO)_6]$. Electrospray mass spectra of **C1−4** in CH_2Cl_2 solution show parent peaks of formula $[Re_2(\mathbf{L})Br(CO)_6]^+$. The isotopic abundance of the parent ions, showing the typical peak separation of a singly charged species, is attributed to the dissociation of one bromine ligand in the mass spectrometer. Although three IR absorption bands ($\upsilon_{C\equiv O}$) are characteristic for the facial coordination of the CO ligands of the rhenium complexes, only two strong IR absorption bands are observed at ~2020 and 1900 cm^{-1} for **C1−4**.[25] When compared to the starting material $[ReBr(CO)_5]$, the shift in CO absorption (**C1−4**: Δ 12−60 cm^{-1}) can be ascribed to the better σ donor and weaker π acceptor of the bipyridine moieties. As expected, the ^1H NMR spectra of the Re(I) helicates are well resolved, indicating the diamagnetic nature of the complexes. However, all spectra show two sets of resonances, which can be assigned to the two diastereomers of the helicates (vide infra).

Others have reported isolation of double- and triple-stranded helicates by spontaneous resolution of racemic mixtures[26] and chromatographic separation,[27] but there is no example on chiral single-stranded helicate. We attempted to isolate the helicates from the diastereomeric mixtures. With repeated recrystallization, using diffuse diethyl ether into a 4:1 CH_2Cl_2/EtOH mixture of the crude complexes, major stereoisomers of **C2** and **C3** were obtained (14 and 16%, respectively). With crude complex **C4**, which has a higher ratio of isomer, the major stereoisomer could be obtained at 50% recovery by a single recrystallization. However, for complex **C1**, the result was unsatisfactory; using the same method, recrystallization of the crude mixture gave only a 1:1 mixture. Apart from recrystallization, with complex **C3** isolation of the diastereomers by column chromatography was attempted. The neutral **C3** complex while stable in silica column for a certain period of time, decomposed gradually. The major and minor stereoisomers appeared as two very close yellow bands (R_f difference of 0.05). Using petroleum ether and ethyl acetate as eluent, the first elution band of **C3**, identified as the major diastereomer by ^1H NMR spectroscopy, was obtained in 15% yield. Because of the overlapping of bands, yield for the minor stereoisomer was only 3%. For **C1**, the major stereoisomer was obtained by column chromatography with 12% yield. These purified single-stranded helicates were characterized by NMR, circular dichroism (CD), and UV−vis spectroscopies only.

Solution Behavior of Bis-Rhenium Complexes. The solution characterizations of bis-rhenium(I) complexes were examined by NMR, CD, and electronic absorption and emission spectroscopies. The ^1H and ^{13}C NMR spectra of all crude single-stranded Re helicates show two sets of resonances. Figure 2 shows an example of crude **C2**. Protons signals at δ 7.6, 8.1, and 8.4 ppm are split into two doublets. In the ^{13}C NMR spectrum, aromatic carbon signals δ121.7, 123.5, 133.1, 135.9, 139.2, 154.1, 160.9, and 161.9 ppm appear as pairs. The two sets of resonances are assigned to the two diastereomers of the complex. The diastereomeric excesses (de) of **C1−4** were determined by some of the well-resolved resonances. For example: **C1**, δ 0.73/0.81 ppm; **C2**, δ 0.76/0.77 ppm; **C3**, δ 4.09/4.25 ppm; and **C4**, δ 0.86/0.89 ppm. While the de's of complexes **C1**, **C2**, and **C3** are in the range of 10−15%, a higher induction of 60% de is observed for complex **C4**. In comparison, higher selectivities are observed for the dinuclear double-stranded helicates of Cu(I) and Ag(I) ions.[15]

Figure 3a−d shows the ^1H NMR spectra of the purified helicates. The C_2-symmetry of the ligands is preserved in each of the helicates. The Re helicates are very stable, as there is no racemization of pure helicates in NMR studies. Unambiguous assignments of resonances of purified **C1−4** are made by gCOSY $^1H-^1H$ NMR experiments (For an example of **C2**, see Figure S1 in the Supporting Information).

Some protons of ligands experience significant changes upon coordination to rhenium. The shifts of H^7 in **C2**, H^{10} in **C3**, and H^7 and H^{13} in **C4** are $\Delta\delta$ 0.56, $\Delta\delta$ 1.05, $\Delta\delta$ 0.67, and $\Delta\delta$ 0.18 ppm, respectively. These protons, which lie in the deshielding region of CO ligands of rhenium complex, experience strong shielding effect upon metal complexation. In the aromatic region, upfield shifts of 0.2−0.3 ppm are observed for ortho or para protons H^4, $H^{4'}$, and H^6, while downfield shifts of 0.2−0.4 ppm are observed for the meta protons H^3 and $H^{3'}$. In examining the helical

(25) (a) Hevia, E.; Pérez, J.; Riera, V. *Inorg. Chem.* **2002**, *41*, 4673. (b) Xue, W.-M.; Chan, M. C.-W.; Su, Z.-M.; Cheung, K.-K.; Liu, S.-T.; Che, C.-M. *Organometallics* **1998**, *17*, 1622. (c) Gelling, A.; Olsen, M. D.; Orrell, K. G.; Osborne, A. G.; Šik, V. *J. Chem. Soc., Dalton Trans.* **1998**, 3479. (d) Gelling, A.; Orrell, K. G.; Osborne, A. G.; Šik, V. *J. Chem. Soc., Dalton Trans.* **1998**, 937.

(26) Sun, Q.; Bai, Y.; He, G.; Duan, C.; Lin, Z.; Meng, Q. *Chem. Commun.* **2006**, 2777.

(27) (a) Hannon, M. J.; Meistermann, I.; Isaac, C. J.; Blomme, C.; Aldrich-Wright, J. R.; Rodger, A. *Chem. Commun.* **2001**, 1078. (b) Khalid, S.; Rodger, P. M.; Rodger, A. *J. Liq. Chromatogr. Relat. Technol.* **2005**, *28*, 2995.

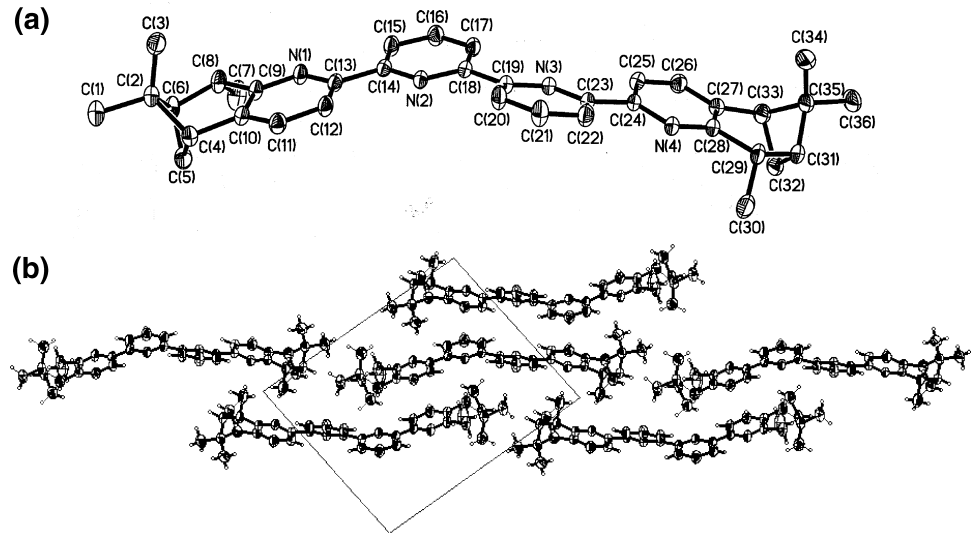

Figure 1. (a) ORTEP diagram of **L4** with labeling scheme. H atoms have been omitted for clarity. (b) Crystal packing of **L4** viewed along axis *b*.

Scheme 2. Synthesis of Single-Stranded Bisrhenium Complexes **C1**−**4**

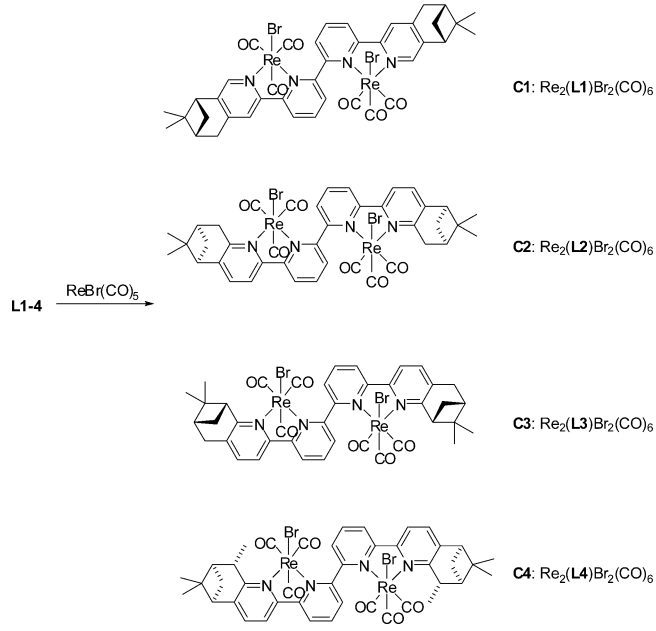

structure, the meta protons $H^{5'}$, which are close to the interannular C−C bond between the two bipyridine domains and hence are expected to be especially sensitive to conformational change, show upfield shifts of 0.19−0.27 ppm (significant shifts of proton resonances of major **C1**−**4** and minor **C3** are summarized in Table S1 in the Supporting Information). These upfield shifts of $H^{5'}$ are also observed in double-helical Cu(I) and Ag(I) complexes.[15] In comparison between the two diastereomer of **C3**, protons $H^{5'}$ show almost identical peak shift compared with the free ligand. This indicates that the aromatic protons experience a similar coordination environment of the two Re centers in the helical structure.

The helical nature of **C1**−**4** in solution was examined by CD spectroscopy. The CD spectra of ligands **L1**−**4** do not show strong absorption, which is due to freely rotated C−C bonds between pyridyl rings. The crude complexes **C1**−**3**, which comprise two diastereomers in an approximate 1:1

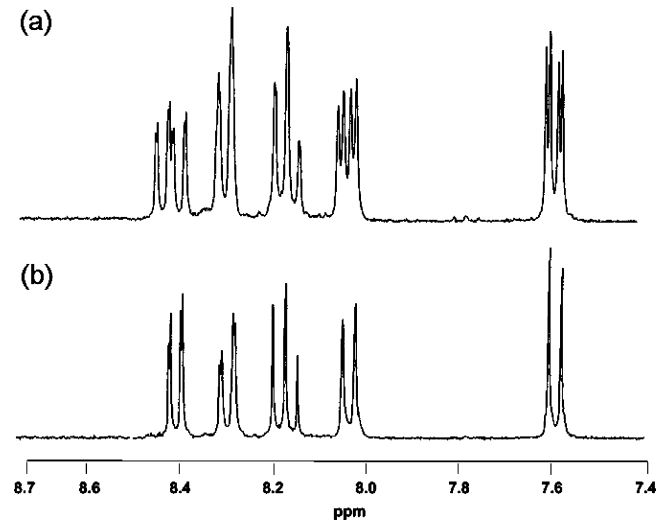

Figure 2. Partial ^{1}H NMR spectra of (a) crude **C2** (b) purified **C2** in $CDCl_3$.

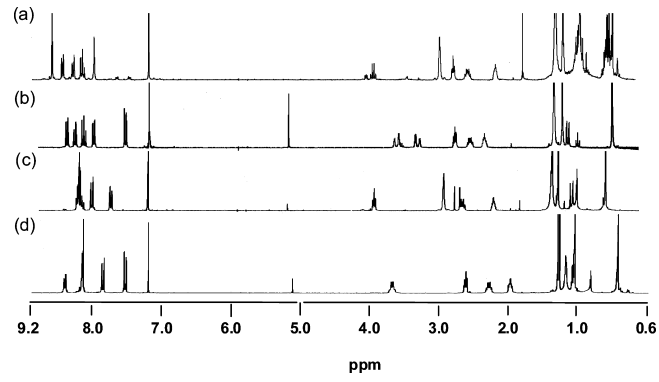

Figure 3. ^{1}H NMR spectra of major stereoisomer of pure (a) **C1**; (b) **C2**; (c) **C3**; (d) **C4**.

ratio, also do not show absorption. Only **C4** shows weak sinoidal CD absorption at 308 nm ($\Delta\varepsilon = 5.4\ M^{-1}\ cm^{-1}$). In contrast, all of the pure Re complexes exhibit typical bisignate curve in the region of 280−350 nm (Figure 4). We have assigned the electronic transitions centered at ca. 330 nm for all the complexes to be $\pi-\pi^*$ bipyridine intraligand transitions (vide infra). The electric transition

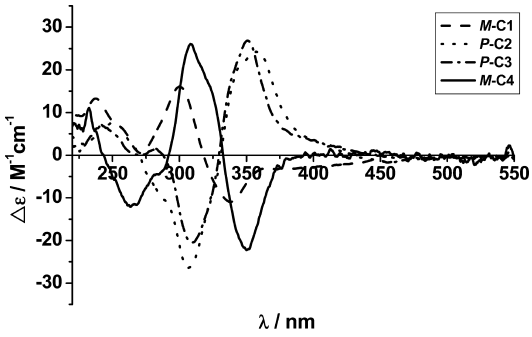

Figure 4. CD spectra of stereomerically pure **C1**−**4** recorded in CH_2Cl_2 with a concentration of 1.0×10^{-6} mol L^{-1}.

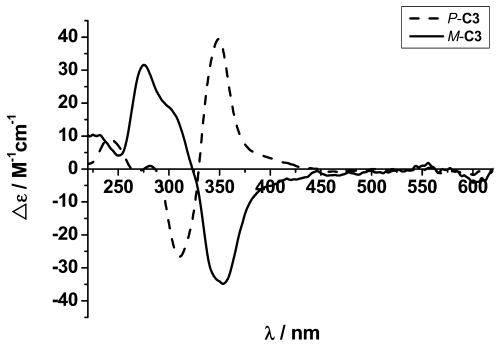

Figure 5. CD spectra of *P*- (major) and *M*-**C3** (minor diastereomers) in CH_2Cl_2 with concentration 1.35×10^{-5} mol L^{-1}.

dipole moment within each chromophore, i.e. half of the helicates or a [ReBr(bpy)$(CO)_3$] moiety, are polarized in the direction of the long axis of the bipyridine. We believe the exciton doublets in the CD spectra originate from the coupling of these long-axis polarized transitions.[28,29]

The exciton chirality for the complexes can be evaluated by determining the dihedral angles between the long axes of the bipyridines from the crystal structures.[28] In a right-handed coordinate system, the dihedral angles between the long axes for complexes *P*-**C2** and *P*-**C3** are 135.8° and 132.0°, respectively, suggesting that positive exciton chirality is established for these complexes. On the other hand, they are −127.8° and −145.0° for complexes *M*-**C1** and *M*-**C4**, revealing that they possess negative exciton chirality. Significantly, these findings are consistent with the Cotton effect observed in their CD spectra: positive first Cotton effects at ∼350 nm and negative second Cotton effects at ∼330 nm are observed in the spectra for *P*-**C2** and *P*-**C3**, and negative first and positive second Cotton effects are observed for *M*-**C1** and *M*-**C4**. The two pure stereomers, *P*-(major) and *M*-configured (minor), of **C3** exhibit *pseudo*-mirror images with absorptions at 311 and 349 nm of similar amplitude (Figure 5). The CD spectra of all purified helicates remained unchanged for 4 days, suggesting no racemization or interconversion between two stereomers has occurred and that the helical integrity and configuration are stable in solution. These stability results are in good agreement with the NMR data.

The electronic absorption and emission properties of **C1**−**4** were examined at 298 K. (for an example, see Figure S2 in the Supporting Information). The intense absorption at ca. 300−375 nm is assigned to intraligand (IL) transitions since similar absorption bands occurred in the free ligand. On the basis of previous spectroscopic studies on rhenium(I) polypyridine complexes,[30,31] the lower energy absorption at ca. 400 nm, with extinction coefficients on the order of 10^3 dm^3 mol^{-1} cm^{-1}, is assigned to metal-to-ligand charge-transfer (MLCT) transition. In emission study, excitation at λ_{ex} > 350 nm at 298 K gives rise to an intense orange-red luminescence at 578−591 nm. The data is consistent with other rhenium(I) polypyridine complexes.[31] In complex **C3**, the absorption and emission properties of the two diastereomers look similar and do not show difference in terms of λ_{max} and emission intensity.

X-ray Characterizations. Single crystals suitable for X-ray analysis were obtained for complexes **C1**−**4**. Crystals of **C1** were obtained by slow diffusion of diethyl ether into a CH_2Cl_2/C_2H_5OH solution of crude **C1**. As observed by ^1H NMR, crystals obtained contained two stereomers in a 1:1 ratio. A centrosymmetric space group was the best we can assign which is probably because of the pseudo-mirror image nature of the two isomers. The space group of Crystals of **C2**−**4** were obtained from stereomerically pure samples and they are the major stereoisomers.

Figure 6 shows the crystal structures of *P*-**C1**, *P*-**C2**, *P*-**C3**, and *M*-**C4**. In the solid state, all bis-rhenium complexes display a single-helical structure. The chiral quaterpyridine acts as a bridging ligand, and each rhenium metal adopts a distorted octahedral geometry. General aspects of molecular structure in all the crystals are similar. The bipyridine moieties of the tetradentate ligand and two cis CO ligands form the square plane, while the remaining CO and bromide ligands coordinate at the apical positions. The three CO ligands are in facial coordination, and they are in close proximity with the pyridine backbone. The distances of the Re−N bond of **C1**−**4** are within 2.19−2.25 Å, comparable in value to the related [Re(diimine)$(CO)_3$Br] complexes.[32,33] All single-stranded helicates possess C_2-symmetry, as the 2-fold axis is found between the C−C bonds of two bipyridines counterparts. The Re···Re distances of all complexes are ∼5.1 Å, and there is no metal···metal interaction. In absolute configuration of Re helicate, **C2** and **C3** are *P*-handed while **C4** is *M*-handed. For **C1**, two diastereomers are found to be co-re-crystallized in the same unit cell.

It is important to note that strong noncovalent intramolecular interactions are observed within the helical structure. As demonstrated in complex *M*-**C4** (Figure 7), the carbonyl ligands **C37≡O1** and **C40≡O4** are directly over and nearly

(28) (a) Ziegler, M.; von Zelewsky, A. *Coord. Chem. Rev.* **1998**, *177*, 257. (b) Berova, N., Nakanishi, K., Woody, R. W., Eds. *Circular Dichroism: Principles and Applications*; VCH: New York, 2000.
(29) Telfer, S. G.; Tajima, N.; Kuroda, R. *J. Am. Chem. Soc.* **2004**, *126*, 1408.
(30) Juris, A.; Campagna, S.; Bidd, I.; Lehn, J.-M.; Ziessel, R. *Inorg. Chem.* **1988**, *27*, 4007.
(31) Lo, K. K.-W.; Hui, W.-K.; Ng, D. C.-M.; Cheung, K.-K. *Inorg. Chem.* **2002**, *41*, 40.
(32) Yam, V. W.-W.; Yang, Y.; Zhang, J.; Chu, B. W.-K.; Zhu, N. *Organometallics* **2001**, *20*, 4911.
(33) Kurz, P.; Probst, B.; Spingler, B.; Alberto, R. *Eur. J. Inorg. Chem.* **2006**, 2966.

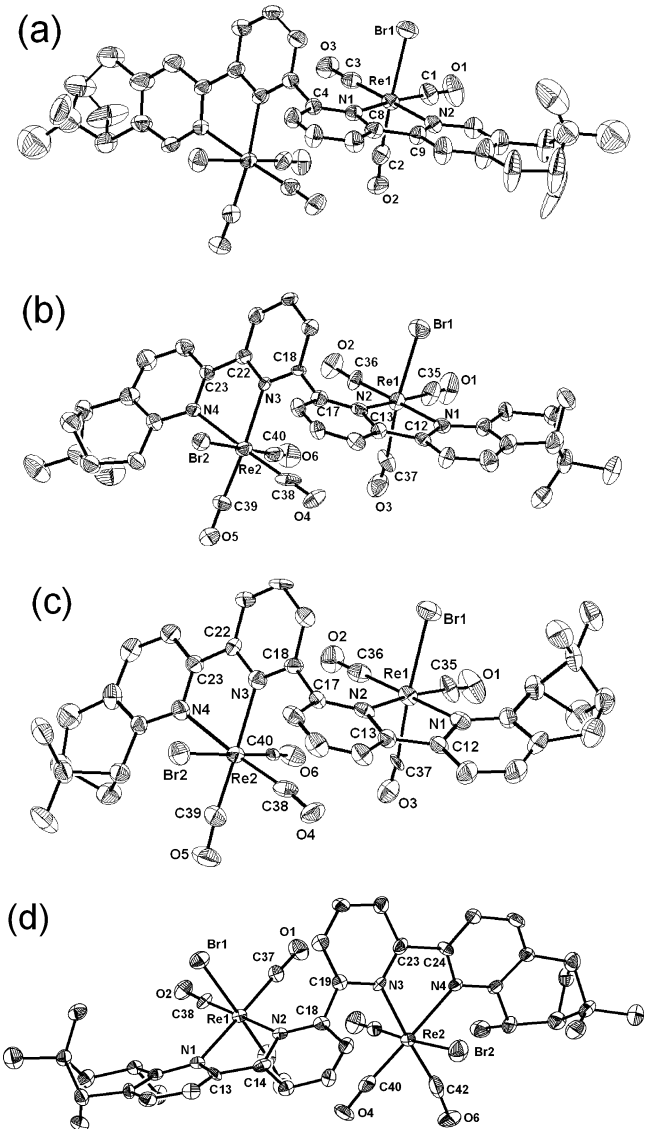

Figure 6. ORTEP drawings of (a) *P*-**C1**, (b) *P*-**C2**, (c) *P*-**C3**, and (d) *M*-**C4** with partial labeling schemes. The thermal ellipsoids are drawn at the 30% probability level. H atoms and solvent molecules are omitted for clarity.

parallel to the adjacent pyridine rings, with short distances of 2.99−3.24 Å. The closeness strongly implies the presence of electrostatic interaction between a permanent dipole and quadrupole,[34] which are also observed in other Re−pyridyl systems.[35,36] Supporting the embrace are CH···Br electrostatic interactions involving the pyridine hydrogen atoms (**H17a** and **H20a**) and the bromine atoms (**Br1** and **Br2**). These interactions have short H···Br distances of 2.867 and 3.002 Å, respectively. All other rhenium single-stranded helicates show electrostatic interactions. The data is summarized in Table 1. The tetrapyridyl rings in each complex are found to be nonplanar. The largest twisting angles of all complexes come from the two central pyridines at 114.25−134.32° (Table 1). Minor twists are found on the terminal pyridyl rings (0.56−24.83°). The overall molecular twist in

(34) Janiak, C. *J. Chem. Soc., Dalton Trans.* **2000**, 3885.
(35) Panda, B. K.; Sengupta, S.; Chakravorty, A. *J. Organomet. Chem.* **2004**, *689*, 1780.
(36) Reger, D. L.; Brown, K. J.; Gardinier, J. R.; Smith, M. D. *J. Organomet. Chem.* **2005**, *690*, 1889.

Table 1. Selected X-ray Data of **C1**−**4**

	P-**C1**	*P*-**C2**	*P*-**C3**	*M*-**C4**
	selected distances, Å			
$\pi_{CO}\cdots\pi_{py}$	3.184	2.99−3.13	3.02−3.06	2.99−3.24
H···Br (intramolecular)	3.01	2.81−2.90	2.94−2.97	2.86−3.00
H···Br (intermolecular)	3.00	2.83	2.86	3.09−3.19
Re···Re	5.09	5.14	5.10	5.25
Br···Br	8.12	8.00	8.11	8.44
	selected angles, deg			
helical twist				
$1^{st}-2^{nd}$ py	3.32	−0.56	2.78	24.83
$2^{nd}-3^{rd}$ py	115.74	117.36	114.25	134.32
$3^{rd}-4^{th}$ py	3.32	9.15	10.27	21.46
overall	122.38	125.95	127.3	180.61

these complexes seems to be in association with the steric hindrance of the chiral groups. The least bulky complex, **C1**, shows an overall helical twist of 122.38° while the most bulky one, **C4**, shows the highest twist of 180.61°.

The intermolecular interactions also play a significant role between helicates in the crystal lattice. Interestingly, the chiral groups of quaterpyridine ligand greatly affect the crystal packing of the single-stranded helicates. The packing diagram of complexes *P*-**C3** in Figure 8 shows stabilization of the single-stranded helicates by intermolecular hydrogen bondings. The short distance **H24a···Br1** of 2.857(1) Å is found mostly between two close single-stranded helicates along the crystallographic *c* axis. As a result, helicates are stacked in layers and held by infinite, strong and multiple hydrogen bondings. The helicates are packed efficiently as no solvent molecules are found within the lattices.

The molecular units of complexes *M*-**C4** are also arranged into chains by H···Br interactions. Figure 9 displays the

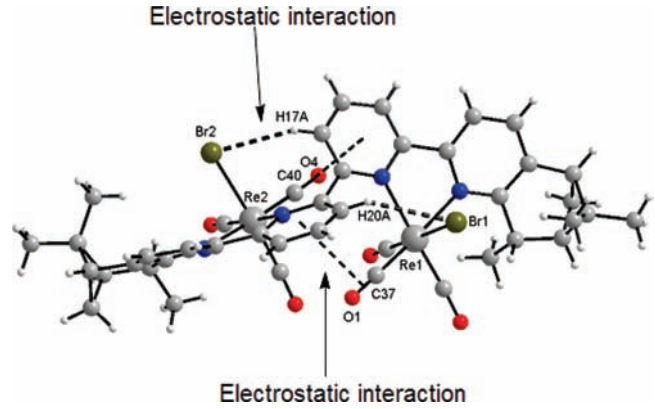

Figure 7. Crystal structure of *M*-**C4**, with a partial atom labeling scheme, showing four electrostatic interactions within the helicate. Solvent molecules are omitted for clarity.

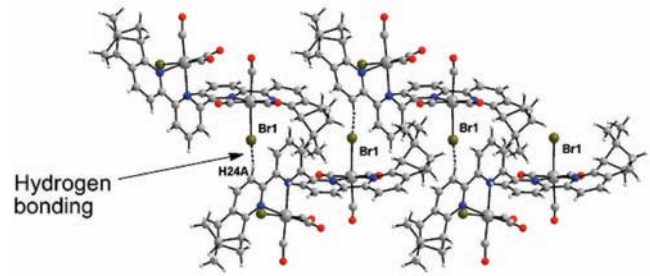

Figure 8. Crystal packing of *P*-**C3**. Hydrogen bondings are found between **Br1** and **H24a**.

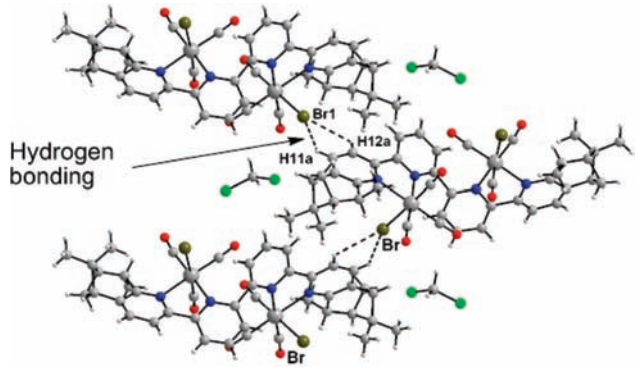

Figure 9. Crystal packing of *M*-**C4**. Hydrogen bondings are found between **Br1** and **H11a** and **H12a**.

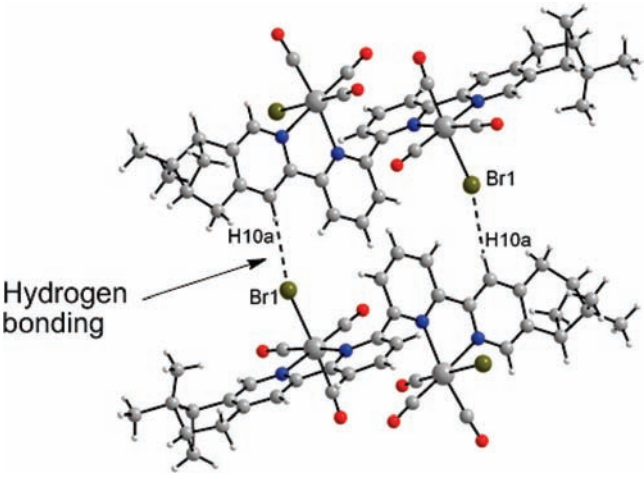

Figure 10. Crystal packing of *P*- and *M*-**C1**. Hydrogen bondings are found between **Br1** and **H10a**.

crystal packing of **C4**, each helicate interacting with the adjacent unit via hydrogen bondings from the Br atom to the third and fourth position of pyridine protons (bond distances of **H11a···Br1** and **H12a···Br1**: 3.093(3) and 3.287(4) Å, respectively) along the *a*-axis. In this case, the single-stranded polymer is formed in a zigzag arrangement with CH_2Cl_2 molecules filling in the cavities, although no strong interactions are observed between solvent molecules and the helicates.

In contrast, no polymeric structure is observed for **C2**. The molecular units of **C2** only have single intermolecular hydrogen bonding (see Figure S3 in the Supporting Information). The solvent molecules such as diethyl ether and ethanol are incorporated for efficient packing.

Figure 10 shows the crystal packing of **C1**, where two diastereomers, *P*-**C1** and *M*-**C1**, with opposite isomer of **L1** are found to cocrystallized in the same unit cells, which is in achiral centrosymmetric space group *C*2/*c*. The crystal structure is not well-resolved, as indicated by the bond distance of **C14···C20**, at 1.729 Å longer than usual for a C−C bond. The two molecules are formed as a dimer and held strongly by two hydrogen bondings (**H10a···Br1**: 2.997 Å). Although opposite absolute configuration of the ligand is observed, the synthetic method is unambiguous and the absolute configurations of the ligand should follow from (*R*)-(+)-myrtenal. Moreover, NMR studies indicate the bulk samples should consist of *P*/*M* stereomers of **C1** only. Thus, although crystallographic studies give centrosymmetric space group, it seems to indicate that the chiral centers are not clearly distinguished and result in a disordered structure. In order to reconfirm the chirality of the helicates, the crystals are redissolved in $CDCl_3$ and an identical NMR spectrum is observed when compared with crude mixture of **C1**. This confirms the presence of two diastereomers in the crystals, instead of a racemic mixture. Corecrystallization of diastereomers have been observed in chiral mononuclear Re complexes before.[37]

Density Functional Theory (DFT) Calculations and Selectivities Studies. All chiral ligands induce selectivities, with **L4** giving the highest ratio of 80:20. The selectivities obviously arise from the rigid chiral groups of the ligand strand. In examining the whole helical structure, there are six stereoisomers possible depending on the handedness (*P*/*M*) of the helix and absolute configuration (syn/anti) of metal chirality, which is induced by the relative positions of bromide ligand to dimethyl groups. In this work, however, we only observe one pair of stereoisomers. We believe that the strong noncovalent interactions established within the helicates are responsible for the stable helical structure in solution and the strong preference of some isomers over others. Although we are not able to obtain crystal structures of the minor stereoisomers, we believe it is the pseudo-mirror image of the major isomer. The fact that CD spectra of the two isolated stereoisomers of **C3** show a pseudo-mirror image and ^{1}H NMR spectra show a similar upfield shift of $H^{5'}$ of **C1**−**4** supports the argument. DFT calculations on both the major and minor isomers of **C4** have been performed in order to determine their relative stability. Frequency calculations have also been performed on these complexes, and the optimized geometries and frequencies data have been summarized in the Supporting Information. The optimized geometry of the major isomer of **C4** is in satisfactory agreement with its crystal structure: the average Re−N, Re−C, and Re−Br bond distances calculated are 2.24, 1.92, and 2.63 Å, respectively, which are close to those determined by X-ray crystallography (2.25, 1.89, and 2.60 Å, respectively). For the optimized structure of the minor isomer, it possesses a single-helical structure as the major isomer, with an anti configuration of Re centers (i.e., two bromide atoms located at the opposite sides of the dimethyl groups (C11 and C12), but at the same side of C13 of the chiral ligand (Figure 11)). Extensive electrostatic interactions are possible in supporting the helical structure just like the major isomer, but close distances are observed between the methyl groups (C13) of **L4** and the bromide ligands (with **H13a···Br1** distance as short as 2.69 Å). Interestingly, the major isomer is only 0.204 kcal mol^{-1} more stable than the minor isomer, which suggested that the proposed structure of the minor isomer is highly likely.

(37) Bosch, W. H.; Englert, U.; Pfister, B.; Stauber, R.; Salzer, A. *J. Organomet. Chem.* **1996**, *506*, 273.
(38) (a) Telfer, S. G.; Sato, T.; Kuroda, R. *Angew. Chem.* **2004**, *116*, 591. Telfer, S. G.; Sato, T.; Kuroda, R. *Angew. Chem.* **2004**, *43*, 581. (b) Telfer, S. G.; Kuroda, R. *Chem.—Eur. J.* **2005**, *11*, 57.

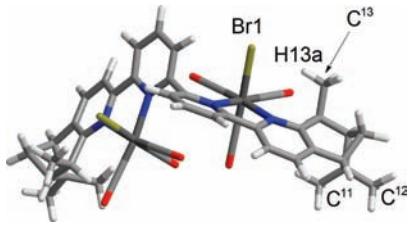

Figure 11. DFT model of the minor diastereomer of **C4** with an anti configuration of Re centers (C light gray; H white; O red; Br yellow; N blue; Re medium gray).

Discussion

The combination of linear polypyridine ligands with neutral Re(I) complexes leads to the preferential formation of a series of single-helical dinuclear complexes, which represents the simplest class of helical polynuclear complexes. In minimizing the steric hindrance between two rhenium centers, a helical twist is established between two bipyridine moieties of the ligand strand. The helical integrity of the isolated complexes is very stable in solution; NMR spectra of pure diastereomers do not show increase in signals of opposite isomers or broadening of resonances, and CD spectra of pure diastereomers neither change nor reduce in absorption intensity at room temperature for a few days.

It is noteworthy that the nonconvalent electrostatic interactions are all important in the formation of the secondary structure. They also play a very important role in the transmission of chiral information between ligands, metal centers, and helicates and between one unit to another. The configurations of rhenium centers (as determined by the relative positions of bromine atoms) are predetermined by the ligand chirality. The helical chirality is further established based on the configuration of the metal center. In this sense, the two rhenium centers are able to communicate with each other and, more importantly, the chiral information is transmitted from the ligand, through the metal, to the helix. This transmission of chiral information in artificial inorganic complexes is reminiscent of many biomolecules, such as α-helix and single-stranded RNA, where the helix formation is based on numerous hydrogen bondings and $\pi-\pi$ interactions and the chiral information is transmitted from one end to another. The transfer of chiral information through hydrogen bondings has also been reported in dinuclear double-stranded helicates.[39]

The chiral information stored in one rhenium helicate can also be transmitted to another, again, by extensive nonconvalent interactions (electrostatic interactions and hydrogen bondings). In this intermolecular recognition process, the formation is strongly influence by the chiral groups of ligands. Only complex **C3** and **C4** form homochiral, two-dimensional polymers. Such molecular recognition-directed self-organization has led to well-ordered, novel supramolecular entities with impressive chiral architectural complexity. Although, in our studies, incomplete diastereoselectivities of helices are observed with **L1**−**4**, pure single-stranded helicates with stable configuration can still be obtained. We believe this facile and effective strategy in the synthesis of configurationally well-defined helical systems can be applied in the construction of various chiral functionalized coordination systems, such as supramolecular materials and chiral catalysts.

(39) (a) Perdew, J. P.; Burke, K.; Ernzerhof, M. *Phys. Rev. Lett.* **1996**, *77*, 3865. (b) Adamo, C.; Barone, V. *J. Chem. Phys.* **1999**, *110*, 6158.

Conclusion

In summary, we have developed a series of novel chiral single-stranded Re(I) helicates with quaterpyridine ligands (**L1**−**4**). Diastereomerically pure Re helicates can be obtained through repeated recrystallization and column chromatography. The two diastereomerically pure single-stranded helicates are configurationally stable in solution, which is very important for applications which require pure stereoisomer. The incorporation of configurationally well-defined helical systems in metallosupramolecular architectures and their use as asymmetric catalysts are under active investigation.

Experimental Section

Chemicals and Starting Materials. All air-sensitive manipulations were carried out under an atmosphere of dry dinitrogen. The solvents used for synthesis were of analytical grade. Toluene was distilled under dinitrogen over sodium. Dichloromethane and acetonitrile were distilled under dinitrogen over calcium hydride. All starting chemicals were of reagent grade quality and were obtained commercially and used as received without further purification.

Physical Measurements and Instrumentation. Infrared spectra in the range 500−4000 cm^{-1} as KBr plates were recorded on a Perkin-Elmer Model FTIR-1600 spectrometer. UV−vis spectra were measured on a Hewlett-Packard 8452A ultraviolet visible diode array spectrophotometer. ^1H and ^{13}C NMR spectra were recorded using a Varian YH300 300 MHz NMR spectrometer. The ^1H chemical shift was referred to TMS as reference. Electrospray (ESI) mass spectra were measured by a PE SCIEX API 365 LC-MS/MS system. Elemental analyses were performed on a Vario EL elemental analyzer. CD spectra were recorded on a Jasco J-715 spectropolarimeter with a 0.1 cm cell at 25 °C, and the results are given in $\Delta\varepsilon$ (M^{-1} cm^{-1}).

Crystal Structure Determination. Crystallographic data for ligand **L4** and single-stranded helicates **C1**−**4** were tabulated in Tables S2 and S3 in the Supporting Information. All intensity data were collected at 293 K on a Bruker Axs SMART 1000 CCD area detector using graphite-monochromated Mo Kα radiation (λ = 0.71073 Å). All collected frames were processed with the software SAINT, and absorption correction was applied (SAD-ABS) to the collected reflections. The structure of the complex was solved by direct methods (SHELXTL) in conjunction with standard difference Fourier syntheses. All non-hydrogen atoms were assigned with anisotropic displacement parameters. The hydrogen atoms were generated in their idealized positions and allowed to ride on the respective carbon atoms.

DFT Calculations. DFT calculations were performed on both the major and minor isomers of **C4**. Their electronic ground states were optimized without symmetry constraints using the density functional PBE1PBE,[39] which is a hybrid of the Perdew, Burke, and Ernzerhof exchange and correlation functional and 25% HF exchange. The Stuttgart small core relativistic effective core potentials were employed for Re atoms with their accompanying basis sets.[40] The 6-31G basis set was employed for C, H, N, and

6-31G*, for Br.[41] Tight SCF convergence (10^{-8} au) was used for all calculations. Frequency calculations were performed on these complexes. As no imaginary vibrational frequencies have been encountered, the optimized stationary points are confirmed to be local minima. All the DFT calculations were performed using the Gaussian 03 program package (revision D.01).[42] Optimized geometries and frequencies data are summarized in the Supporting Information.

Synthesis of 2-Bromo-(6-pyridinioacetyl) Pyridine Iodide 1. To a pyridine solution (5 mL) of 2-bromo-6-acetylpyridine (8 mmol, 1.61 g) was added a solution of iodine (8 mmol, 2.03 g) in pyridine (5 mL). The mixture was heated at 110 °C for 3 h and, after cooling, the dull yellow solid was filtered and washed with cold ethanol. This product was characterized by ^{1}H NMR and IR. Yield 80% (2.60 g). ^{1}H NMR (300 MHz, DMSO): δ 6.46 (s, 2H), 8.11 (s, 3H), 8.29 (t, 2H, J = 6.9 Hz), 8.75 (t, 1H, J = 7.2 Hz), 8.97 (d, 2H, J = 6.6 Hz). IR (KBr, υ cm^{-1}): 3022.9 vs, 2969.5 vs, 2946.6 vs, 1719.6 vs, 1635.7 s, 1491.1 s, 1344.5 s.

General Procedure for Synthesis of Chiral Bipyridine Ligands 2a−d. 2-Bromo-(6-pyridinioacetyl) pyridine iodide (2 mmol, 0.81 g), α,β-unsaturated ketone (6 mmol) and ammonium acetate were dissolved in glacial acetic acid (2.7 mL). The mixture was stirred under reflux (120 °C) overnight. The reaction was quenched by addition of saturated $NaHCO_3$. The mixture was extracted with diethyl ether (three times by 50 mL) and dried with $MgSO_4$ and filtered. The solvent was removed under reduced pressure and the brown residue obtained was purified by column chromatography. Products were characterized by ^{1}H NMR and ESI-MS.

General Procedure for Synthesis of Bipyridine 2a. The above procedure was followed using (*R*)-(+)-myrtenal. Workup and purification by column chromatography with light petroleum ether-ethyl acetate (20:1, R_f = 0.3) gave bipyridine **2a** (0.33 g, 50%). ^{1}H NMR (300 MHz, $CDCl_3$): δ 0.65 (s, 3H), 1.23 (d, 1H, J = 9.3 Hz), 1.42 (s, 3H), 2.31−2.35 (m, 1H), 2.68−2.75 (m, 1H), 2.87 (t, 1H, J = 5.4 Hz), 3.06 (d, 2H, J = 2.7 Hz), 7.46 (d, 1H, J = 7.8 Hz), 7.65 (t, 1H, J = 7.8 Hz), 8.19 (s, 2H), 8.33 (d, 1H, J = 7.8 Hz). ESI-MS *m*/*z*: 331 (M^+ + 1).

General Procedure for Synthesis of Bipyridine 2b. The above procedure was followed using (1*R*)-(+)-pinocarvone. Workup and purification by column chromatography with light petroleum ether-ethyl acetate (20:1, R_f = 0.3) gave bipyridine **2b** (0.36 g, 55%). ^{1}H NMR (300 MHz, $CDCl_3$): δ 0.67 (s, 3H), 1.30 (d, 1H, J = 9.6 Hz), 1.42 (s, 3H), 2.38−2.43 (m, 1H), 2.67−2.74 (m, 1H), 2.82 (t, 1H, J = 5.4 Hz), 3.17 (d, 2H, J = 2.7 Hz), 7.32 (d, 1H, J = 7.8 Hz), 7.42 (d, 1H, J = 7.8 Hz), 7.63 (d, 1H, J = 7.8 Hz), 8.08 (d, 1H, J = 7.5 Hz), 8.34 (d, 1H, J = 7.5 Hz). ESI-MS *m*/*z*: 331 (M^+ + 1).

General Procedure for Synthesis of Bipyridine 2c. The above procedure was followed using (−)-nopinone. Workup and purification by column chromatography with light petroleum ether-ethyl acetate (20:1, R_f = 0.3) gave bipyridine **2c** (0.34 g, 52%). ^{1}H NMR (300 MHz, $CDCl_3$): δ 0.67 (s, 3H), 1.32 (d, 1H, J = 9.9 Hz), 1.43 (s, 3H), 2.31−2.35 (m, 1H), 2.70−2.77 (m, 1H), 2.97 (d, 2H, J = 2.4 Hz), 3.06 (t, 1H, J = 5.7 Hz), 7.42 (dd, 1H, J = 7.8, 0.9 Hz), 7.52 (d, 1H, J = 8.1 Hz), 7.59 (t, 1H, J = 7.8 Hz), 8.16 (d, 1H, J = 7.8 Hz), 8.34 (dd, 1H, J = 7.5, 0.9 Hz). ESI-MS *m*/*z*: 331 (M^+ + 1).

General Procedure for Synthesis of Bipyridine 2d. The above procedure was followed using (*R*)-(−)-isopinocampheol. Workup and purification by column chromatography with petroleum ether-ethyl acetate (20:1, R_f = 0.3) gave bipyridine **2d** (0.40 g, 58%). ^{1}H NMR (300 MHz, $CDCl_3$): δ 0.65 (s, 3H), 1.30 (d, 1H, J = 9.9 Hz), 1.41 (s, 3H), 1.44 (d, 3H, J = 6.9 Hz), 2.13−2.18 (m, 1H), 2.53−2.60 (m, 1H), 2.80 (t, 1H, J = 5.4 Hz), 3.18−3.26 (m, 1H), 7.30 (d, 1H, J = 7.8 Hz), 7.41 (d, 1H, J = 7.5 Hz), 7.62 (d, 1H, J = 7.5 Hz), 8.07 (d, 1H, J = 7.5 Hz), 8.40 (d, 1H, J = 7.8 Hz). ESI-MS *m*/*z*: 345 (M^+ + 1).

General Procedures for Synthesis of Quaterpyridine L1−4. To a solution of $NiCl_2 \cdot 6H_2O$ (3 mmol, 0.72 g) in degassed DMF (15 mL) at 70 °C under N_2, triphenylphosphine (12 mmol, 3.2 g) was added to give a blue solution. Zinc powder (6.5 mmol, 0.44 g) was then added and the resulting mixture was stirred for 1 h, which resulted in the formation of a dark-brown mixture. Chiral bipyridine ligand (2.5 mmol) in degassed DMF (2.5 mL) was added slowly and the mixture was stirred for another 3 h. The mixture was then allowed to cool to room temperature and 25% aqueous NH_3 (25 mL) was added. The layers were separated, and the aqueous layer was extracted with CH_2Cl_2 (three times by 35 mL). The combined organic layers were washed with water (three times by 35 mL). Drying with $MgSO_4$ and removal of the solvent under reduced pressure yielded a pale yellow solid. The obtained solid was purified by column chromatography or recrystallization. Products were characterized by ^{1}H, ^{13}C NMR, CHN, IR and MS analyses.

Quaterpyridine L1. The above procedure was followed using **2a**. The crude product was acidified with HCl (6M, 10 mL), and the aqueous layer was extracted with diethyl ether (three times by 20 mL). The aqueous layer was then neutralized with NaOH, and the resulting solution was extracted with CH_2Cl_2 (three times by 50 mL). Drying with $MgSO_4$ and removal of the solvent under reduced pressure yielded a pale yellow solid. The solid was recrystallized from ethanol to give white solids. Yield 60% (0.40 g). ^{1}H NMR (300 MHz, $CDCl_3$): δ 0.69 (s, 6H), 1.28 (d, 2H, J = 9.6 Hz), 1.44 (s, 6H), 2.36−2.37 (m, 2H), 2.70−2.77 (m, 2H), 3.13 (s, 4H), 7.99 (t, 2H, J = 7.8 Hz), 8.24 (s, 2H), 8.44 (t, 2H, J = 8.1 Hz), 8.45 (s, 2H), 8.65 (d, 2H, J = 8.1 Hz). ^{13}C NMR ($CDCl_3$): δ 21.64, 26.27, 32.10, 33.30, 39.53, 40.44, 44.84, 120.76, 120.86, 120.96, 137.90, 143.27, 145.54, 145.73, 154.83, 155.69, 156.15. Anal. calcd. for $C_{34}H_{34}N_4$: C, 81.88; H, 6.89; N, 11.23. Found: C, 81.72; H, 6.82; N, 10.98%. IR (KBr): 2925.0 vs, 1569.87 vs, 1422.07 vs, 1261.29 s, 1099.22 s, 1077.40 s. ESI-MS *m*/*z*: 499 (M^+ + 1).

Quaterpyridine L2. The above procedure was followed using **2b**. The crude product was acidified with HCl (6M, 10 mL), and the aqueous layer was extracted with ether (three times by 20 mL). The aqueous layer was then neutralized with NaOH, and the

(40) Andrae, D.; Haeussermann, U.; Dolg, M.; Stoll, H.; Preuss, H. *Theor. Chim. Acta* **1990**, *77*, 123.
(41) Hehre, W. J.; Ditchfield, R.; Pople, J. A. *J. Chem. Phys.* **1972**, *56*, 2257.
(42) Frich, M. J.; Trucks, G. W.; Schlegel, H. B.; Scuseria, G. E.; Robb, M. A.; Cheeseman, J. R.; Montgomery, J. A., Jr.; Vreven, T.; Kudin, K. N.; Burant, J. C.; Millam, J. M.; Iyengar, S. S.; Tomasi, J.; Barone, V.; Mennucci, B.; Cossi, M.; Scalmani, G.; Rega, N.; Petersson, G. A.; Nakatsuji, H.; Hada, M.; Ehara, M.; Toyota, K.; Fukuda, R.; Hasegawa, J.; Ishida, M.; Nakajima, T.; Honda, Y.; Kitao, O.; Nakai, H.; Klene, M.; Li, X.; Knox, J. E.; Hratchian, H. P.; Cross, J. B.; Bakken, V.; Adamo, C.; Jaramillo, J.; Gomperts, R.; Stratmann, R. E.; Yazyev, O.; Austin, A. J.; Cammi, R.; Pomelli, C.; Ochterski, J. W.; Ayala, P. Y.; Morokuma, K.; Voth, G. A.; Salvador, P.; Dannenberg, J. J.; Zakrzewski, V. G.; Dapprich, S.; Daniels, A. D.; Strain, M. C.; Farkas, O.; Malick, D. K.; Rabuck, A. D.; Raghavachari, K.; Foresman, J. B.; Ortiz, J. V.; Cui, Q.; Baboul, A. B.; Clifford, S.; Cioslowski, J.; Stefanov, B. B.; Liu, G.; Liashenko, A.; Piskorz, P.; Komaromi, I.; Martin, R. L.; Fox, D. J.; Keith, T.; Al-Laham, M. A.; Peng, C. Y.; Nanayakkara, A.; Challacombe, M.; Gill, P. M. W.; Johnson, B.; Chen, W.; Wong, M. W.; Gonzalez, C.; Pople, J. A. *Gaussian 03*, revision D.01. Gaussian, Inc.: Wallingford, CT, 2004.

resulting solution was extracted with CH_2Cl_2 (three times by 50 mL). Drying with $MgSO_4$ and removal of the solvent under reduced pressure yielded a pale yellow solid. The solid was recrystallized from ethanol to give white solids. Yield 72% (0.45 g). ^{1}H NMR (300 MHz, $CDCl_3$): δ 0.71, (s, 6H), 1.35 (d, 2H, J = 9.6 Hz), 1.45 (s, 6H), 2.41−2.46 (m, 2H), 2.70−2.77 (m, 2H), 2.85 (t, 2H, J = 5.7 Hz), 3.23 (d, 2H, J = 3.0 Hz), 7.40 (d, 2H, J = 7.8 Hz), 7.97 (t, 2H, J = 7.8 Hz), 8.35 (d, 2H, J = 7.5 Hz), 8.51 (d, 2H, J = 7.8 Hz), 8.64 (d, 2H, J = 7.8 Hz). ^{13}C NMR ($CDCl_3$): δ 21.25, 25.98, 31.86, 36.60, 39.45, 40.15, 40.19, 46.39, 117.72, 120.14, 120.38, 137.33, 141.94, 141.97, 153.38, 155.12, 155.54, 156.03. Anal. calcd. for $C_{34}H_{34}N_4 \cdot H_2O$: C, 79.04; H, 7.02; N, 10.84. Found: C, 78.94; H, 6.93; N, 10.65%. IR (KBr): 2922.50 s, 1557.60 vs, 1421.19 vs, 1104.14 s, 798.15 s, 764.97s. ESI-MS m/z: 499 ($M^+ + 1$).

Quaterpyridine L3. The above procedure was followed using bipyridine **2c**. The crude product was acidified with HCl (6M, 10 mL,) and the aqueous layer was extracted with ether (three times by 20 mL). The aqueous layer was then neutralized with NaOH, and the resulting solution was extracted with CH_2Cl_2 (three times by 50 mL). Drying with $MgSO_4$ and removal of the solvent under reduced pressure yielded a pale yellow solid. The solid was recrystallized from ethanol to give white solids. Yield 72% (0.45 g). ^{1}H NMR (300 MHz, $CDCl_3$): δ 0.72 (s, 6H), 1.38 (d, 2H, J = 9.9 Hz), 1.46 (s, 6H), 2.38−2.40 (m, 2H), 2.73−2.80 (m, 2H), 3.01 (d, 4H, J = 2.7 Hz), 3.12 (t, 2H, J = 5.7 Hz), 7.59 (d, 2H, J = 7.8 Hz), 7.95 (t, 2H, J = 7.8 Hz), 8.42 (d, 2H, J = 7.5 Hz), 8.44 (dd, 2H, J = 7.8, 0.9 Hz), 8.63 (dd, 2H, J = 7.8, 0.9 Hz). ^{13}C NMR ($CDCl_3$): δ 21.32, 26.03, 30.90, 31.31, 39.22, 40.10, 50.38, 118.96, 120.50, 120.89, 130.73, 136.08, 137.68, 152.01, 155.39, 159.90, 165.75. Anal. calcd. for $C_{34}H_{34}N_4$: C, 81.89; H, 6.87; N, 11.24. Found: C, 81.65; H, 6.84; N, 11.21%. IR (KBr): 2930.37 s, 1563.74 vs, 1429.23 vs, 1112.79 m, 804.15 s. ESI-MS m/z: 499 ($M^+ + 1$).

Quaterpyridine L4. The above procedure was followed using bipyridine **2d**. The crude product was acidified with HCl (6M, 10 mL), and the aqueous layer was extracted with ether (three times by 20 mL). The aqueous layer was then neutralized with NaOH, and the resulting solution was extracted with CH_2Cl_2 (three times by 50 mL). Drying with $MgSO_4$ and removal of the solvent under reduced pressure yielded a pale yellow solid. The solid was recrystallized from ethanol to give white solids. Yield 80% (0.50 g). ^{1}H NMR (300 MHz, $CDCl_3$): δ 0.70 (s, 6H), 1.37 (d, 2H, J = 9.9 Hz), 1.45 (s, 6H), 1.51 (d, 6H, J = 7.2 Hz), 2.18−2.23 (m, 2H), 2.57−2.64 (m, 2H), 2.85 (t, 2H, J = 5.7 Hz), 3.26−3.33 (m, 2H), 7.38 (d, 2H, J = 7.8 Hz), 7.97 (t, 2H, J = 7.8 Hz), 8.34 (d, 2H, J = 7.5 Hz), 8.51 (d, 2H, J = 8.1 Hz), 8.64 (d, 2H, J = 7.8 Hz). ^{13}C NMR ($CDCl_3$): δ 18.31, 20.99, 26.42, 28.71, 39.01, 41.55, 46.98, 47.34, 117.94, 120.39, 120.68, 133.50, 137.57, 142.15, 153.61, 155.52, 156.13, 160.22. Anal. calcd. for $C_{36}H_{38}N_4$: C, 82.01; H, 7.21; N, 10.63. Found: C, 81.63; H, 7.13; N, 10.32%. IR (KBr): 2929.88 s, 1557.60 vs, 1432.25 vs, 816.58 s, 790.78 s. ESI-MS m/z: 527 ($M^+ + 1$).

General Method for Preparation of Single-Stranded Re(I) Helicates. [$ReBr(CO)_5$] (90 mg, 0.21 mmol) and quaterpyridine ligand (0.1 mmol) were dissolved with stirring in a mixture of benzene (30 mL) and tetrahydrofuran (7 mL) and the solution was heated under reflux for 18 h. Light petroleum ether (bp 40−60 °C, 50 mL) was added to the cooled reaction mixture to precipitate a yellow solid. The solid was filtered and further washed with light petroleum ether and dried in vacuo. The product was characterized by ^{1}H NMR, ^{13}C NMR, IR, ESI-MS, and elemental analysis. Further purification was carried out through recrystallization using diffuse diethyl ether into a 4:1 CH_2Cl_2/EtOH mixture of the crude complex.

[Re_2(L1)Br_2($CO)_6$], C1. Yellow crystals. IR (KBr, υ_{max} cm^{-1}): 2919 m, 2853 m, 2023 s, 1900 s, 1450 m. ESI-MS m/z: 1119 ($M - Br)^+$. Anal. calcd. for $C_{40}H_{34}N_4O_6Br_2Re_2 \cdot 0.5H_2O \cdot 0.5CH_2Cl_2$: C: 38.90; H, 2.91; N, 4.48. Found: C, 38.78; H, 2.92; N, 4.47. UV−vis (CH_2Cl_2): λ_{max} nm (ε dm^3 mol^{-1} cm^{-1}) = 272 (68 300), 346 (51 600). Fluorescence (CH_2Cl_2): λ_{max} nm = 584.

[Re_2(L2)Br_2($CO)_6$], C2. Yellow crystals. IR (KBr, υ_{max} cm^{-1}) 2930 m, 2034 m, 1964 s, 1598 m. ESI-MS m/z: 1119 ($M - Br)^+$. Anal. calcd. for $C_{40}H_{34}N_4O_6Br_2Re_2 \cdot 0.5(H_2O) \cdot 0.5(CH_2Cl_2)$: C: 38.90; H, 2.91; N, 4.48. Found: C, 38.74; H, 2.92; N, 4.39. UV−vis (CH_2Cl_2): λ_{max} nm (ε dm^3 mol^{-1} cm^{-1}) = 263 (68 200), 344 (54 300). Fluorescence (CH_2Cl_2): λ_{max} nm = 589.

[Re_2(L3)Br_2($CO)_6$], C3. Yellow crystals. IR (KBr, υ_{max} cm^{-1}): 2929 m, 2848 m, 2028 m, 1895 s, 1419 m. ESI-MS m/z: 1119 ($M - Br)^+$. Anal. calcd. for $C_{40}H_{34}N_4O_6Br_2Re_2$: C: 40.07; H, 2.86; N, 4.67. Found: C, 40.32; H, 2.86; N, 4.65. UV−vis (CH_2Cl_2): λ_{max} nm (ε dm^3 mol^{-1} cm^{-1}) = 262 (71 200) (major); 262 (68 900) (minor), 344 (55 900) (major); 341 (52 600) (major). Fluorescence (CH_2Cl_2): λ_{max} nm = 591 (major); 592 (minor).

[Re_2(L4)Br_2($CO)_6$], C4. Yellow crystals. IR (KBr, υ_{max} cm^{-1}): 2924 m, 2023 m, 1900 m, 1424 m. ESI-MS m/z: 1147 ($M - Br)^+$. Anal. calcd. for $C_{42}H_{38}N_4O_6Br_2Re_2 \cdot 0.5CH_2Cl_2$: C, 40.21; H, 3.10; N, 4.41. Found: C, 40.02; H, 3.09; N, 4.40. UV−vis (CH_2Cl_2): λ_{max} nm (ε dm^3 mol^{-1} cm^{-1}) = 265 (73 500), 346 (54 100). Fluorescence (CH_2Cl_2): λ_{max} nm = 578.

Acknowledgment. Financial support from the Hong Kong Research Grants Council GRF grant (CityU 101108) and City University of Hong Kong SRG grant (7002223) are gratefully acknowledged.

Supporting Information Available: Figures S1−S3 and Tables S1−S7. This material is available free of charge via the Internet at http://pubs.acs.org.

IC802249F